



**Field of studies: Geoinformation**

**Album ID: 455828**

**Tomasz Matuszek**

**Measuring an impact of the Landsat 8 thermal  
band on the supervised land cover classification  
results**

*Ocena wpływu zastosowania kanału termalnego  
Landsat na wyniki nadzorowanej klasyfikacji pokrycia  
terenu*

Engineer's thesis written  
in the Institute of Geoecology and Geoinformation  
under the supervision of  
dr. hab. Jakub Nowosad

Poznań, 2023



# **Abstract**

## **Abstrakt**

Streszczenie powinno przedstawać skrótnie główny problem pracy i jego rozwiązań. Możliwa struktura streszczenia to: (1) 1-3 zdania wstępne do problemu (czym się zajmujemy, dlaczego jest to ważne, jakie są problemy/luki do wypełnienia), (2) 1 zdanie opisujące cel pracy, (3) 1-3 zdania przedstawiające użyte materiały (dane) i metody (techniki, narzędzia), (4) 1-3 zdania obrazujące główne wyniki pracy, (5) 1-2 zdania podsumowujące; możliwe jest też określenie dalszych kroków/planów.

Słowa kluczowe: (4-6 słów/zwrotów opisujących treść pracy, które nie wystąpiły w tytule)

## **Abstract**

The abstract must be consistent with the above text.

Keywords: (as stated before)

# Contents

|  |           |
|--|-----------|
| <b>Abstract</b>  | <b>3</b>  |
| <b>1 Introduction</b>  | <b>5</b>  |
| <b>2 Materials and methods</b>                                     | <b>7</b>  |
| 2.1 Satellite imagery . . . . .                                    | 9         |
| 2.2 Land cover data . . . . .                                      | 10        |
| 2.3 Machine learning . . . . .                                     | 13        |
| 2.4 Variable importance and its spatial distribution . . . . .     | 17        |
| 2.5 R language environment . . . . .                               | 21        |
| <b>3 Result of the model - land cover map</b>                      | <b>23</b> |
| <b>4 Assessing model quality</b>                                   | <b>27</b> |
| <b>5 Evaluation of thermal band's impact on prediction results</b> | <b>29</b> |
| 5.1 Overall importance of thermal band . . . . .                   | 29        |
| 5.2 Spatial distribution of thermal band's importance . . . . .    | 30        |
| <b>6 Conclusion</b>  | <b>33</b> |
| <b>Bibliography</b>  | <b>35</b> |

# **Chapter 1**

## **Introduction**

- applications and relevance of land cover maps
  - machine learning and supervised classification of satellite images as a tool for creating land cover maps
  - pointing out that thermal band if often omitted in land cover classification models, exact impact of thermal factor isn't fully clear
  - goal of the thesis is to create land cover map of Poznań metropolitan area and measure the impact of thermal band on the model results
- 

Wprowadzenie powinno mieć charakter opisu od ogólnego do szczegółów (np. trzy-pięć paragrafów). Pierwszy paragraf powinien być najbardziej ogólny, a kolejne powinny przybliżać czytelnika do problemu. Przedostatni paragraf powinien określić jaki jest problem (są problemy), który praca ma rozwiązać i dlaczego jest to (są one) ważne.

Wprowadzenie powinno być zakończone stwierdzeniem celu pracy. Dodatkowo tutaj może znaleźć się również krótki opis co zostało zrealizowane w pracy.

Pisząc ten rozdział proszę pomyśleć o osobach, które zupełnie nie znają opisywanej tematyki. Należy tutaj krok po kroku wyjaśnić podstawowe koncepcje, istotność problemu,

wyniki poprzednich podobnych badań, itd. Ten rozdział obejmuje tylko kwestie, które już zostały wykonane przez inne osoby - nowe wyniki mają swoje miejsce w rozdziale **?@sec-wyniki.**

Każda kwestia opisana w tym rozdziale powinna być cytowana. Dodatnie cytowania odbywa się poprzez uzupełnienie pliku `thesis.bib` zapisem w formacie BibTeX, a następnie dodanie nazwy referencji poprzedzonej znakiem `@`. Przykładowo, zacytowanie książki *Geocomputation with R* odbywa się poprzez (Lovelace et al., 2019).

W przypadku, gdy cytowanie zostało poprawnie wpisane oraz istnieje w pliku `thesis.bib` to bibliografia powinna się automatycznie wygenerować na końcu pracy.

W przypadku, gdy praca dyplomowa opisuje konkretny obszar to można po tym rozdziale stworzyć kolejny rozdział opisujący “obszar badań”.

Ten i kolejne rozdziału moją mieć także podrozdziały. Tworzenie podrozdziałów polega na stworzeniu nowej linii rozpoczynającej się od znaków `##` a następnie tytułu podrozdziału. Dodatkowo w postaci `{#sec-}` można dodać skrót nazwy rozdziału/podrozdziału umożliwiający odnoszenie się do niego używając operatora `[ -@sec ]`.

# **Chapter 2**

## **Materials and methods**

Workflow of the study consisted of several stages: preprocessing of source data (described in Sections 2.1 and 2.2), creating training dataset, model's parameters tuning (Section 2.3.2), land cover map prediction, model quality assessment (Section 2.3.3) and evaluating the impact of the thermal band on the model's results (Section 2.4).

Visual representation of the workflow is shown in Figure 2.1.

Each of these steps was performed using R programming language (R Core Team, 2021). Final visualisations were created in QGIS software (QGIS Development Team, 2009). Both programming environment and GIS software used in this process are open-source.

Landsat ARD dataset, provided by GLAD laboratory at the University of Maryland, was used as a source of multi-spectral satellite imagery. Training points were obtained from LUCAS dataset created by Eurostat (d'Andrimont et al., 2020). Both datasets were downloaded for central-western part of Poland which was chosen as training area (Figure 2.2). This data was preprocessed and then used to train the model and validate its performance.

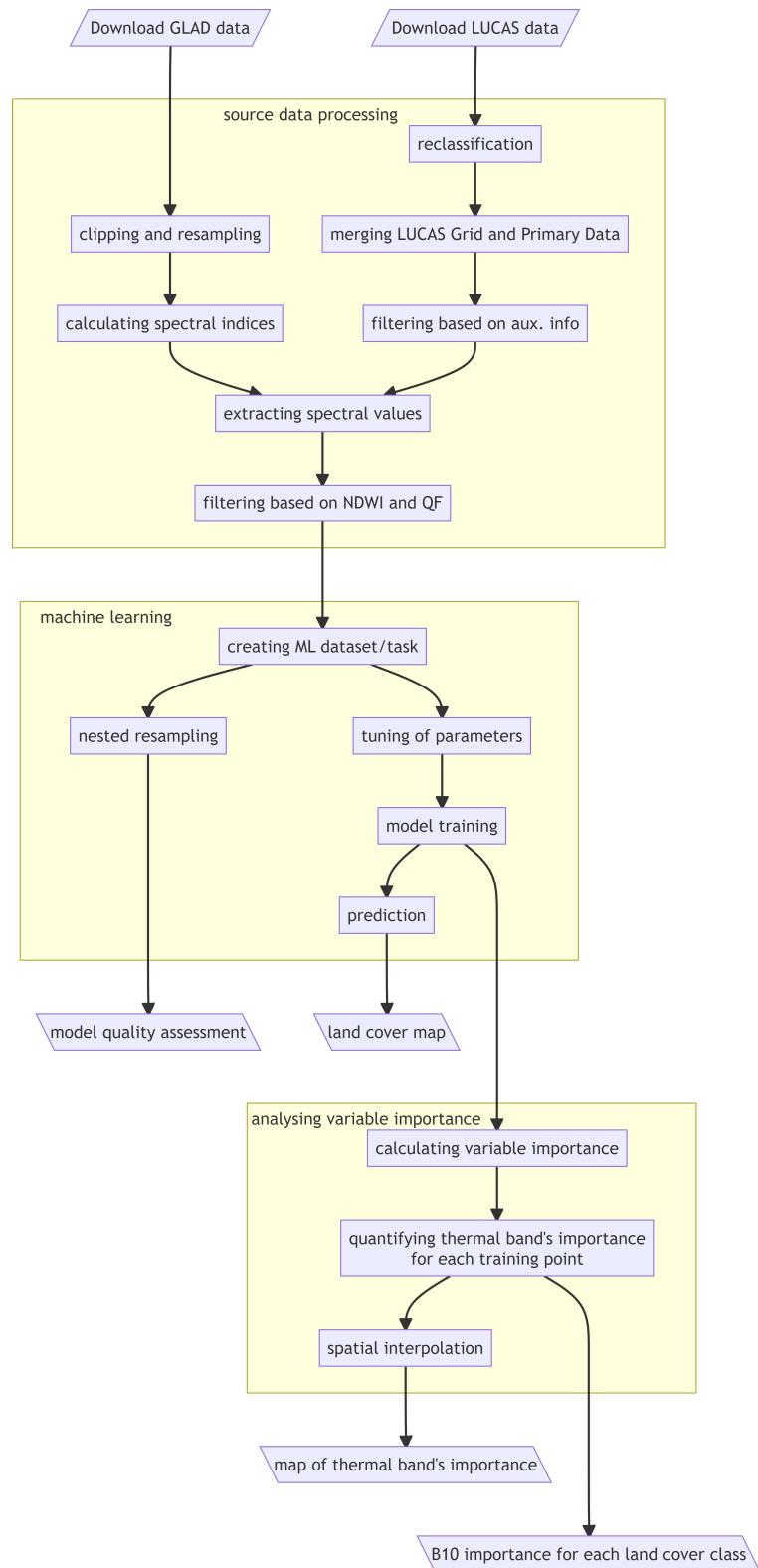


**Figure 2.1:** General workflow of the study

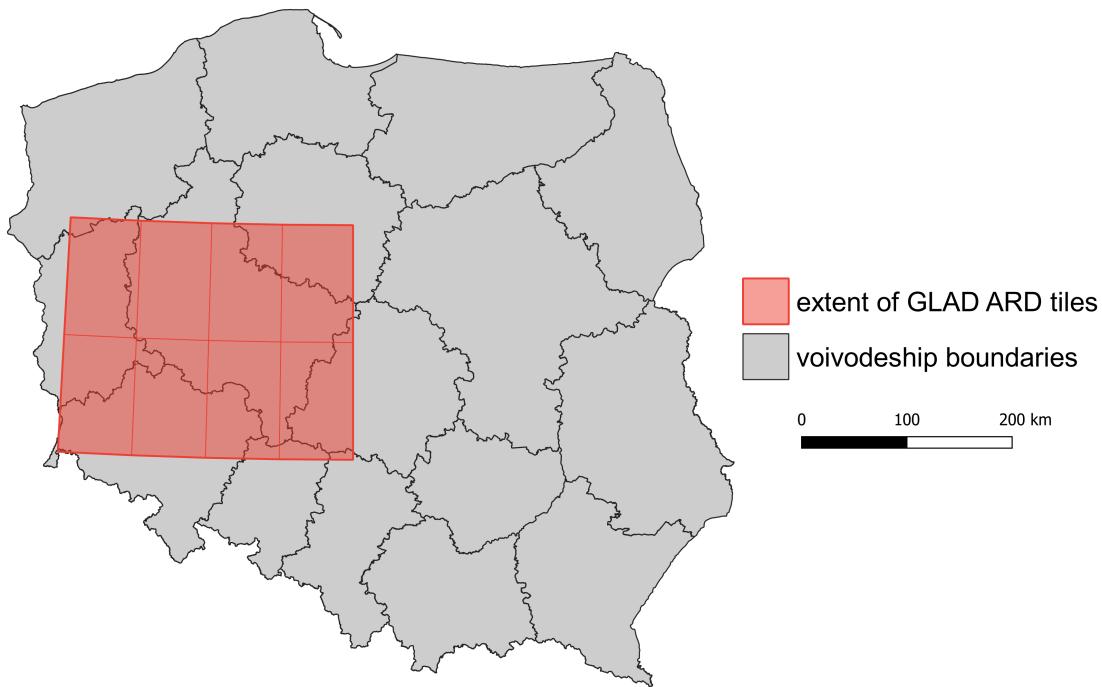


**Figure 2.2:** Area covered by downloaded satellite imagery

## 2.1 Satellite imagery

Satellite imagery from GLAD Landsat ARD product is available in 16-day interval composites and is divided into  $1^\circ \times 1^\circ$  tiles. Processing of original Landsat images performed by GLAD team included converting spectral bands to top-of-atmosphere (TOA) reflectance, converting thermal band to brightness temperature (BT) in Kelvins, scaling the values of all bands, as well as, adding quality flag for every pixel (Potapov et al., 2020).

Satellite images for eight  $1^\circ \times 1^\circ$  tiles, covering the study area (Figure 2.1), were downloaded using GLAD Tools v1.1 and PERL programming language. These images are from 10th interval of the year 2018, so downloaded mosaics consist of images created between 24.05.2018 and 8.06.2018. All downloaded images were merged and reprojected from WGS84 coordinate reference system (EPSG:4326) to UTM zone 33N (EPSG:32633). Every band was also resampled from its original  $0.00025^\circ$  resolution (corresponding to 27.83 m on the equator) to 30 meters.

**Table 2.1:** Formulas of spectral indices derived from Landsat data

| band/index                                 | abbreviation | formula                               |
|--|--------------|---------------------------------------|
| Blue                                       | B2           | -                                     |
| Green                                      | B3           | -                                     |
| Red  | B4           | -                                     |
| Near Infrared                              | B5 (NIR)     | -                                     |
| Short-wave Infrared 1                      | B6 (SWIR1)   | -                                     |
| Short-wave Infrared 2                      | B7 (SWIR2)   | -                                     |
| Thermal                                    | B10 (TIRS1)  | -                                     |
| Normalized Difference Vegetation Index     | NDVI         | (B5 - B4) / (B4 + B5)                 |
| Modified Normalized Difference Water Index | MNDWI        | (B3 - B6) / (B3 + B6)                 |
| Normalized Difference Moisture Index       | NDMI         | (B5 - B6) / (B5 + B6)                 |
| Modified Bare Surface Index                | MBI          | (B6 - B7 - B5) / (B6 + B7 + B5) + 0.5 |

In addition, four spectral indices were derived: Normalized Difference Vegetation Index (NDVI), Modified Normalized Difference Water Index (MNDWI), Normalized Difference Moisture Index (NDMI) and Modified Bare soil Index (MBI). Formulas used to calculate these indices can be found in Table 2.1.

## 2.2 Land cover data

Data collected during LUCAS survey performed by Eurostat was chosen as land cover training set. At the moment of writing, it is the most accurate and comprehensive dataset containing information about land use and land cover (Pflugmacher et al., 2019) due to the fact that every point was either manually photo-interpreted or assessed during an *in-situ* visit.

LUCAS survey consists of two phases. The first phase is based on a grid of points with 2km spacing covering whole territory of the European Union (which equals to more than 1 million points). Each point of the grid is visually interpreted using ortho-photos or satellite images, and classified into one of seven major land-cover classes. These classes are: arable land, permanent crops, grassland, wooded areas/shrub land, bare land, artificial land and water. In the second phase, a subsample of grid points is selected

and then visited by Eurostat surveyors. They classify each point according to full LUCAS land cover and land use classification. The survey takes place in the spring and summer in order to observe chosen places in their high vegetation season (d'Andrimont et al., 2020).

Surveyor not only assign land cover and land use classes to points, but they also add auxillary information such as plant species present at the site, percentage of land coverage of a chosen class, height of the trees and their maturity, as well as information about local water management and irrigation. If there are more than one land cover/land use types at the point, observer can also assign a secondary class for every LUCAS point.

Majority of the training points used in the classification model were from the second phase of LUCAS survey, also called LUCAS Primary Data. I downloaded a total of 4,153 points for the study area. Pre-processing step included omitting records with missing data, excluding artificial linear land cover classes (e.g. roads or railways) and excluding points that were surveyed more than 500 meters from their theoretical location. In the next step, detailed land cover classes were aggregated into eight main groups of land cover types. Two of them - grassland and shrubland were additionally aggregated into one land cover class due to their spectral and descriptive similarity. Then, I filtered some of the points according to the percentage of land cover class coverage or percentage of impervious surface coverage (Table 2.2). This step reduced number of unreliable training points with mixed land cover, e.g. points with assigned class covering less than 50% of surface around it.

For the least frequent classes in the LUCAS Primary Data dataset - bare land, artificial land and water bodies - I also added points classified during the first phase of LUCAS survey (Figure 2.3). This step was necessary to ensure that every land cover class is represented by enough number of points. It was not possible only for wetlands class, because of lack of such category in the first phase classification. At the end of the pre-processing, dataset had 3,778 training points (Buck et al., 2015).

**Table 2.2:** Filters applied to reclassified land cover groups. IMP - impervious surface, HRB - herbaceous plants cover, TC - tree cover

| ID | LC class        | LUCAS Grid           | LUCAS Primary Data               | Filters               |
|----|-----------------|----------------------|----------------------------------|-----------------------|
| 1  | arable land     | -                    | B00 (Cropland)                   | <30% IMP              |
| 2  | grasslands      | -                    | E00 (Grassland), D00 (Shrubland) | >50% HRB;<br><30% IMP |
| 3  | forests         | -                    | C00 (Woodland)                   | >50% TC;<br><20% IMP  |
| 4  | bare land       | 6 (Bare surface)     | F00 (Bare land)                  | -                     |
| 5  | artificial land | 7 (Artificial areas) | A00 (Artificial land)            | >70% IMP              |
| 6  | water bodies    | 8 (Inland water)     | G00 (Water areas)                | -                     |
| 7  | wetlands        | -                    | H00 (Wetlands)                   | -                     |

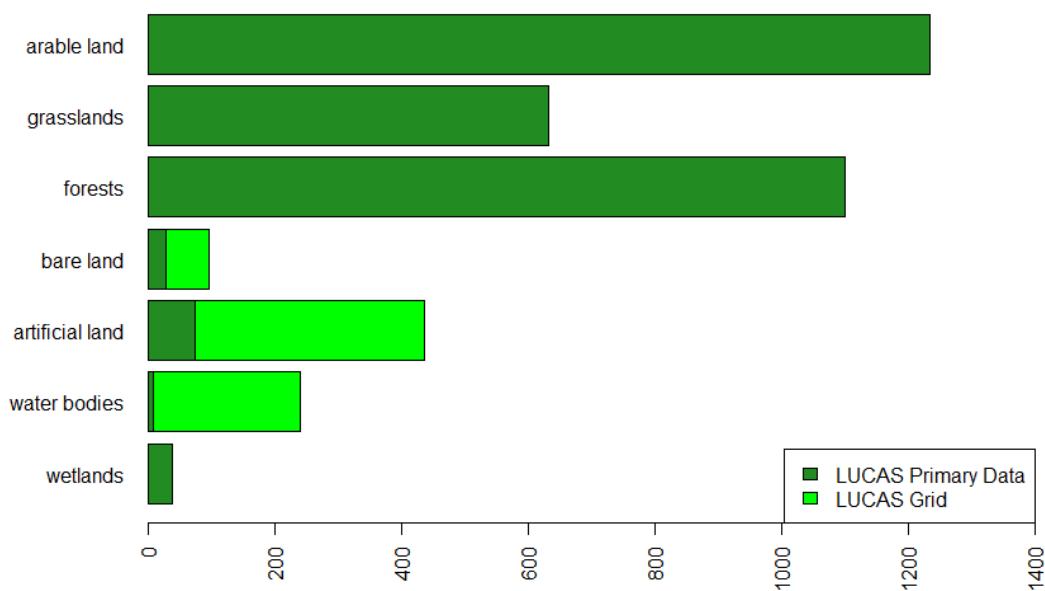


**Figure 2.3:** Distribution of points by land cover class after pre-processing

After extracting values from Landsat ARD raster, LUCAS points were also filtered using quality flag provided. Only points with clear-sky quality flag were taken into account during the model training. Moreover, water bodies points in which NDWI was lower than 0 were also excluded. These two conditions eliminated over 400 points in total.

Training set obtained after pre-processing can be seen in Figure 2.4. Spatial distribution of data points was fairly even and due to the structure of LUCAS data set, every point was located 2 kilometers or further from the next one.

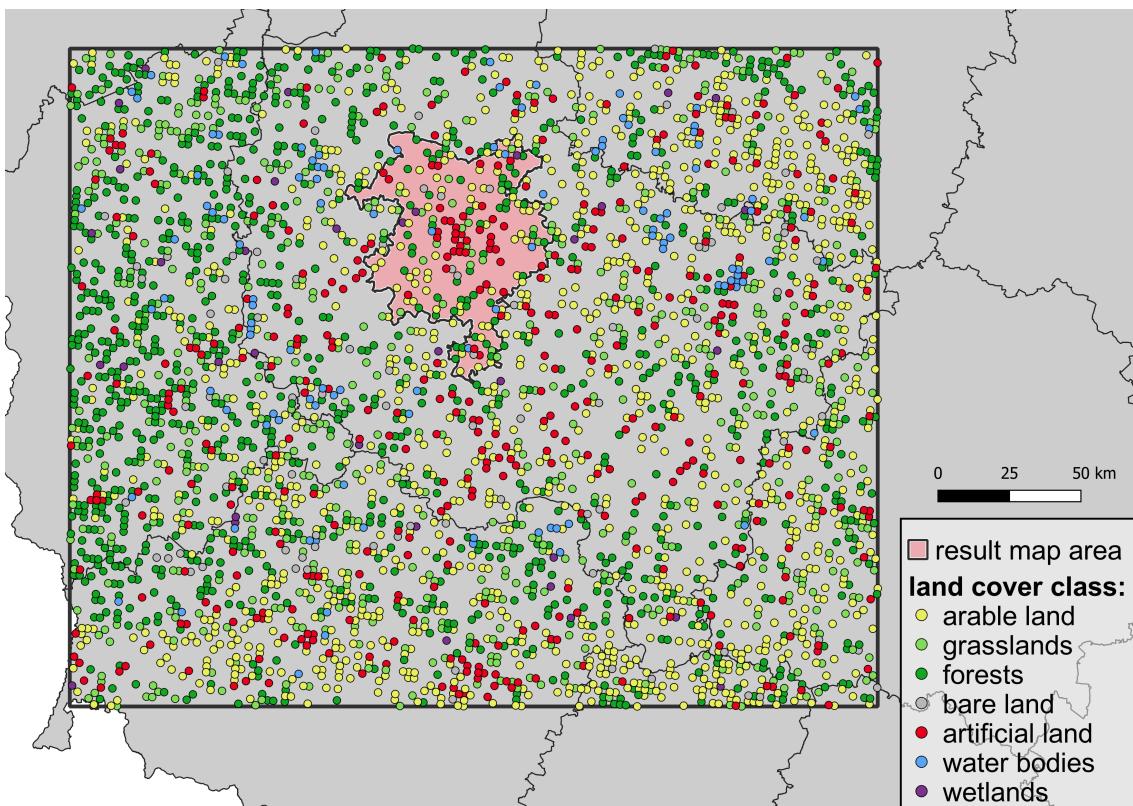


**Figure 2.4:** Spatial distribution of LUCAS training points after pre-processing

## 2.3 Machine learning

Machine learning is a computation method used to teach machines from datasets automatically, without being specifically programmed (Mahesh (2018); Sarker (2021)). We can divide machine learning methods into two main groups: supervised and unsupervised.

Unsupervised learning analyzes unlabeled datasets without the need for human intervention. This is widely used for extracting generative features, identifying meaningful trends and structures, grouping results and exploratory purposes (Sarker, 2021). This type of machine learning discovers hidden patterns or data groupings (clusters) which is used in exploration analysis or objects segmentation.

Supervised learning uses labeled training data and a collection of training examples, which are used by an algorithm to find relationships between different variables. It is carried out when certain goals are identified to be accomplished from a certain set of

inputs. There are two main types of supervised learning tasks: classification (separating data) and regression (fitting data) (Sarker, 2021).

In this study, supervised classification algorithm called Random Forest (RF) was used (Breiman, 2001).

### **2.3.1 Random forest algorithm**

I chose Random Forest as an algorithm used in this study. It is a very popular machine learning tool thanks to its high interpretability and relatively high accuracy (Qi, 2012). Other advantages of this algorithm is its ability to handle missing values, wide spectrum of accepted variable types (continuous, binary, categorical) and ease of modelling high-dimensional data (Qi, 2012). Random Forest consists of a specified number of decision trees, which are based on series of splitting rules.

Decision tree aims to partition the dataset into smaller, more homogeneous groups (Kuhn et al., 2013). This process creates a set of rules by dividing dataset into several categories. Each rule in the decision tree is specified by a feature (variable used to split) and a threshold (value of a feature dividing dataset) (Sekulić et al., 2020). Random forest algorithm is characterized by using many decision trees at the same time and receiving results by applying majority voting system based on outputs of all decision trees (Kuhn et al., 2013). Each tree in the forest has slightly different input data - a subset of data is sampled with replacement to get different result in every tree. This process is known as bagging or bootstrap aggregating (Schonlau et al., 2020). Moreover, algorithm is allowed to use only subset (randomly sampled) of available variables which reduces correlation between trees (Sohil et al., 2022).

### **2.3.2 Parameter tuning**

Random Forest algorithm takes several hyperparameters as an input in order to specify how much should it fit to training data. Optimizing these parameters is crucial for tree-based machine learning models (Yang et al., 2020). Model's hyper-parameters can be fine-tuned to find values that give the best model accuracy. I chose three hyperparameters for tuning: number of trees, maximum depth of the forest and minimal size

**Table 2.3:** Tuned parameters of RF model

| Hyper-parameter | Search space | Optimal value |
|-----------------|--------------|---------------|
| number of trees | 50 - 400     | 272           |
| maximum depth   | 10 - 40      | 20            |
| min. node size  | 1 - 10       | 1             |

of each node in decision tree. Then, 10 models with different hyper-parameter values chosen randomly from specified search space were created and trained. I used overall accuracy achieved by each classifier to rank their performance and choose parameters that train the model the best. Parameters' search spaces and tuning results can be found in Table 2.3.

### 2.3.3 Model quality assessment

Accuracy of the model was assessed using five performance measures:

- Overall accuracy: ratio of number of correct predictions to the total number of input points
- Kappa coefficient: how well the classification performed as compared to randomly assigning values
- Recall (producer's accuracy): how often are real features on the ground correctly shown on the classified map
- Precision (user's accuracy): how often the class on the map will actually be present on the ground
- F1-score: harmonic mean between precision and recall, measures if classifier both classifies data correctly and does not miss a significant number of points

Every above metric, except Kappa coefficient, take values from 0 to 1. Value of 0 means poor model performance and value of 1 means high quality of the model. As for Kappa coefficient, values range from -1 to 1. Values below 0 mean worse agreement between raters than random chance and values above 0 (up to 1) mean model performing better than random.

Values of these indices were estimated with the help of resampling technique called spatial cross-validation (CV). It is a type of cross-validation that divides dataset into folds and also considers spatial aspect of the data.

In  $k$ -fold cross-validation, every data point is used in both training and testing set. Whole dataset is randomly divided into  $k$  equal parts (*folds*). Then, machine learning model is independently trained  $k$  times and in each run, different part of the dataset is used as validation set while remaining  $k - 1$  parts are used to fit the model. This way, every data point is used in the testing set only once and is used to train the model in the remaining runs (Jiao et al., 2016). Usually, whole cross-validation procedure is repeated several times to get higher number of unique dataset splits and to receive more reliable average values of the overall accuracy (Varga et al., 2021). Such approach is a compromise which enables possibility of using a whole dataset in the training process of the final model without a need of acquiring independent testing set.

Since this study is based on geographic data, spatial autocorrelation needs to be taken into account. As Tobler stated: “Everything is related to everything else, but near things are more related than distant things” (Tobler, 1970). In order to prevent testing points from being related to training points, I applied spatial cross-validation approach which aims to prevent the model to overfit to the training data. This method is different than regular cross-validation only in the partitioning step - instead of randomly dividing dataset into groups, location of data points is used together with k-means clustering (Brenning, 2012) in order to create spatially disjoint folds (Lovelace et al., 2019). Thanks to this partitioning method, spatial bias can be significantly reduced which leads to more reliable performance estimation. Example of such approach can be seen on Figure 2.5.

With the aim to determine values of model’s hyperparameters as accurately as possible, I performed nested spatial cross-validation. This method is an extension of previously described approach, with hyperparameter tuning added to the process. Each fold created in the spatial CV is further divided into next  $n$  folds which comprise the tuning level of the process. Then, another cross-validation is performed on these folds in order to determine performance of randomly sampled hyperparameter values. The best hyperparameter combination is chosen to train the model on outer fold on performance



**Figure 2.5:** Comparison of random and spatial partitioning of dataset for cross-validation on external example data (Source: Lovelace et al. (2019))

estimation level (Schratz et al., 2019). Whole process is then repeated on every of  $k$  outer folds which leads to most accurate performance measurement as well as defining the best hyperparameter setting. FIGURE?

## 2.4 Variable importance and its spatial distribution

Quantifying importance of model's variables is a part of evaluating its results. It can be used for model simplification and exploration, domain-knowledge-based validation or knowledge generation (Biecek et al., 2021). This study was focused on the latter purpose since its aim was to check if thermal information has an impact on land-cover classification.

Importance of model variables can be measured on two levels: dataset level and instance level (Biecek et al., 2021). On the dataset level, we can measure change in model's accuracy depending on the presence of one chosen variable (Section 2.4.1). This gives basic knowledge about this variable's impact on model predictions. Assessing importance on the instance level helps to understand an impact of variables for one

specific data point (Section 2.4.2). Moreover, the instance level importance can be utilized to interpolate variable importance values from points into continuous raster data (Section 2.4.3).

### **2.4.1 Dataset level**

Measuring variable importance on the dataset level requires evaluating model twice: once with original data and once with permuted values of the considered variable. The main idea behind this action is to measure difference between models' performance. Breiman ([2001](#)) assumes that if a variable is important, then it is expected to lower model's performance after permuting its values. For this purpose, cross entropy was used as a loss function thus its change was considered as a measure of variable importance ([Biecek et al., 2021](#)). In order to measure each variable's importance, twelve separate models were created: one with original data and eleven modified models, each one with different variable's values permuted. Comparison of these eleven models and original model made possible quantifying impact of every variable on original model's results. This value is treated as overall variable importance on the dataset level.

There is also more visual method to explore variable importance on dataset level. It is based on interpreting partial-dependence (PD) profiles of variables (Figure 2.6). Such type of plot shows how does probability of choosing certain class changes as a function of the selected variable ([Biecek et al., 2021](#)). Values for PD profile are calculated by averaging Ceteris-paribus profiles created for every observation in the dataset. This approach is an easy and intuitive way to understand variables' impact on model results. If probability values of choosing certain class do not change along with changes of variable's value, we can assume that this variable does not have big impact on model predictions or that our model did not detect such dependence.

### **2.4.2 Instance level**

Another way to measure variable importance in machine learning models is the instance level evaluation. It helps to find out how much each variable contributed to the classification result for a particular observation ([Biecek et al., 2021](#)). One way of calculating

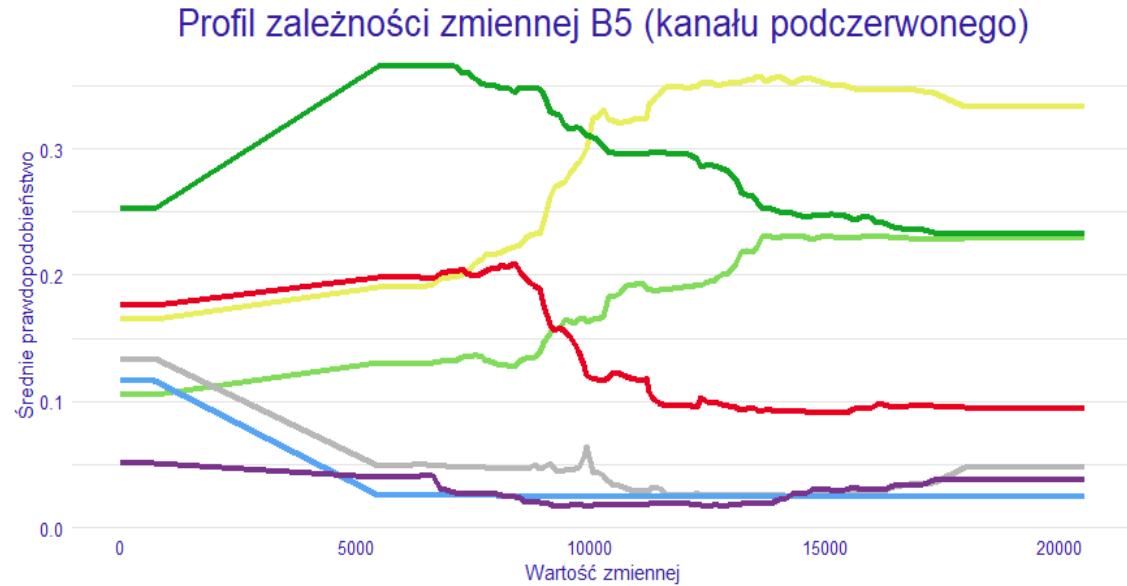


**Figure 2.6:** Example variable profile for near-infrared band (B5).

variable impact on the observation result is creating break-down plot (Figure 2.7). Its main idea is to estimate contribution of variable by measuring the change in model's predictions while fixing the values of consecutive variables to values recorded for the chosen observation (Biecek et al., 2021). After fixing the value of variable for whole dataset, change in model's prediction is calculated. This value indicates variable impact on a chosen observation.

However, above method is highly dependent on variable ordering and interactions between these variables (Biecek et al., 2021). To address this issue, I applied another approach based on averaging values from multiple break-down plots, each one with different ordering of the variables. This method originates from "Shapley values" (Shapley et al., 1953) and was adapted to machine learning by Štrumbelj and Kononenko (2010). Main idea of this approach is to apply several different variable orderings, create a break-down plot for each of them and calculate the mean value of contribution for each variable (Figure 2.8). Thanks to this method, the influence of variable ordering can be mostly removed (Biecek et al., 2021).

Eventually, Shapley values provide a possibility to measure contribution of each variable in every observation in the training set. Such result enables us to add spatial context to the variable importance, which is further described in Section 2.4.3.

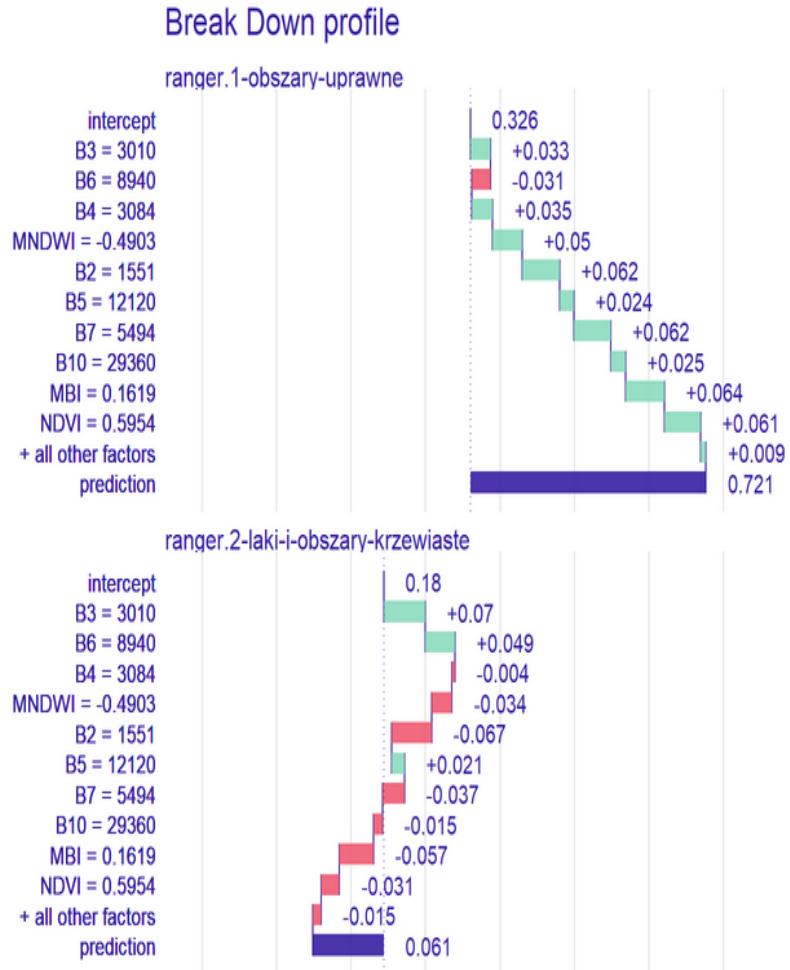


**Figure 2.7:** Example of a break-down plot that visualises variables' impact on chosen observation

### 2.4.3 Spatial distribution

In order to estimate spatial distribution of variable importance values, I applied two different approaches. First of them is based on the raster aggregation - resampling of satellite imagery from 30 m to 1.5 km resolution. Lowering the resolution of the data and averaging bands' values highly decreases computational time, as well as helps to discover more general trends and patterns rather than local ones. After resampling, Shapley values are calculated for every raster cell and variable importance value is quantified.

The second approach utilizes LUCAS training points used during a model training together with spatial interpolation techniques. First, Shapley values are calculated for every

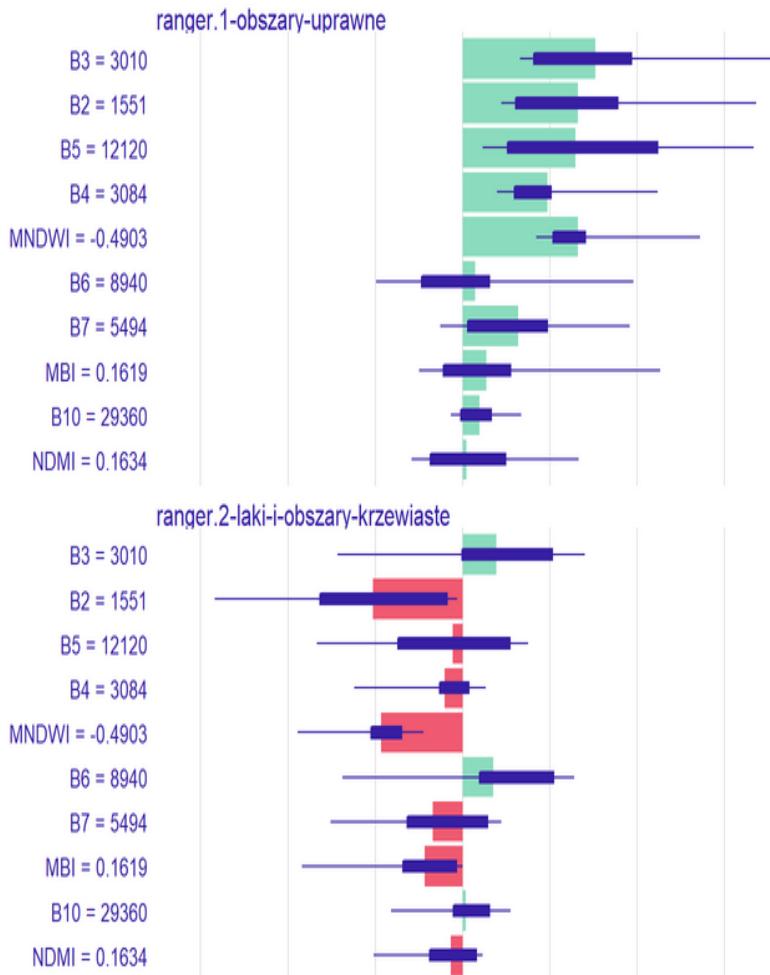


**Figure 2.8:** Example plot of Shapley Additive Explanations

point and importance of variable is assigned to them. This step is followed by spatial interpolation of variable importance values from points to continuous raster layer with the help of the Inverse Distance Weighting (IDW) interpolation method.

Both approaches have their pros and cons. Raster aggregation method is spatially more consistent, but averaging of spectral values may not entirely represent objects on the ground. On the other hand, point interpolation method is very accurate for places near LUCAS points location, but values for more distant objects may not be as reliable.

## 2.5 R language environment

Almost every step of analysis described in previous sections was performed with use of R (R Core Team, 2021) - an open-source programming language designed mainly

for statistical computing and visualizing data. I used RStudio (RStudio Team, 2020) as an integrated development environment (IDE). Apart from base R functionalities, a number of packages created by the R community were implemented into workflow. I used *terra* package (Hijmans, 2022) to perform raster data operations and *sf* (Pebesma, 2022) to manipulate and process vector data. To conduct machine learning steps of the analysis, I used an environment of various machine learning packages called *mlr3* (Lang et al., 2022). Random forest algorithm used by *mlr3* framework is part of the *ranger* package (Wright et al., 2021). I also used *dplyr* (Wickham et al., 2022) and *tidyverse* packages (Wickham, 2021) to clean and process tabular data. *DALEX* (Biecek et al., 2022) and *DALEXtra* (Maksymiuk et al., 2022) packages provided various functionalities enabling me to estimate variable importance and visualize these results with the help of *ggplot2* package (Wickham et al., 2021). Package called *gstat* (Pebesma et al., 2021) helped to interpolate variable importance values from points to a continuous raster layer. In addition, *future* package (Bengtsson, 2021) was used to enable multi-threading of some computationally intensive tasks.

## **Chapter 3**

# **Result of the model - land cover map**

- land cover map of Poznań metropolitan area
- comparison of land cover map and RGB satellite imagery
- probability map of model results

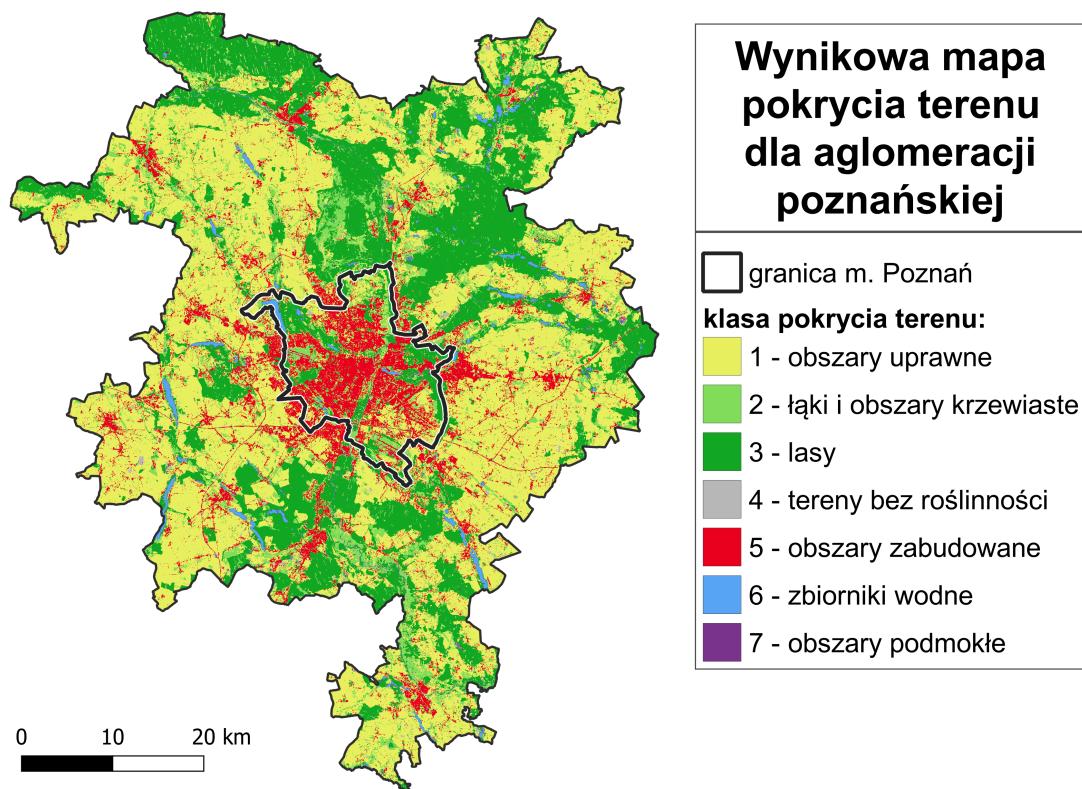


Figure 3.1: Land cover map of Poznań metropolitan area created during this study.

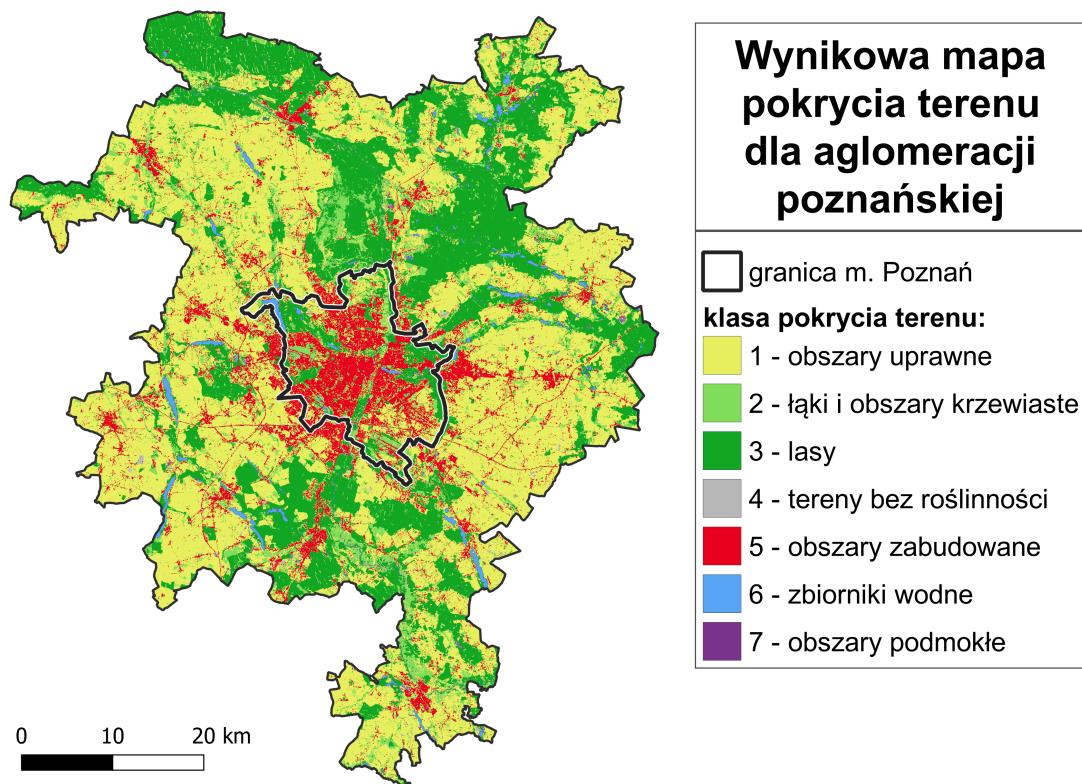
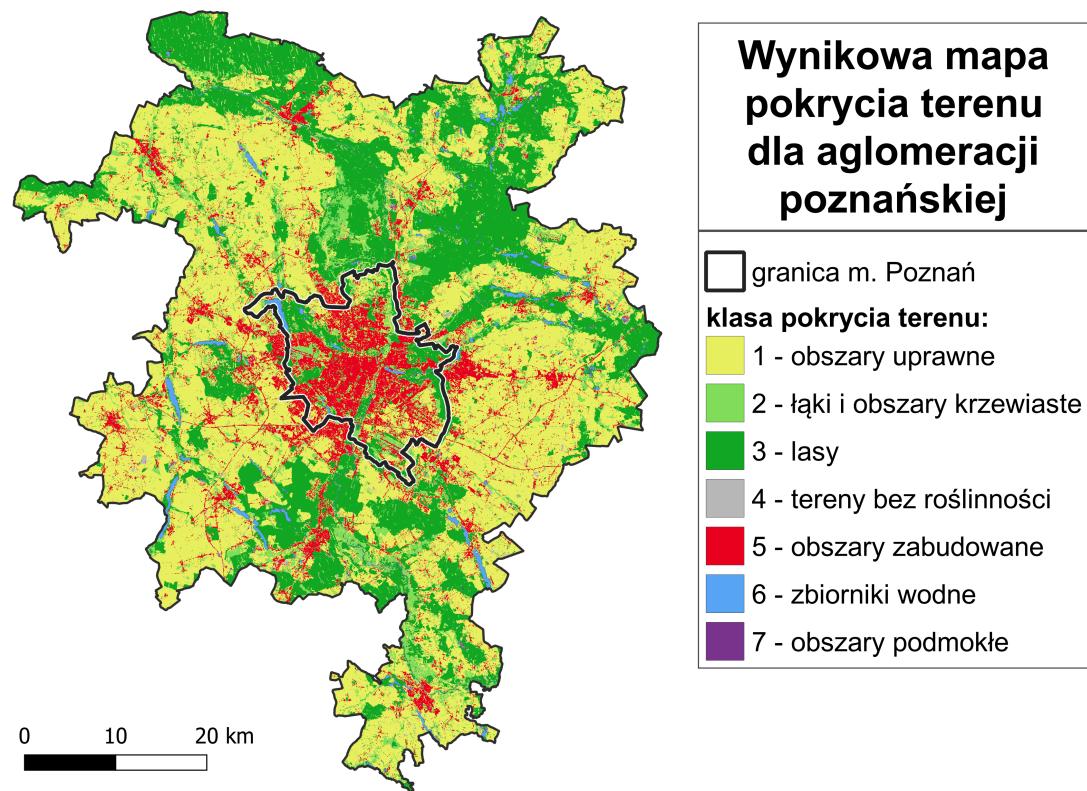


Figure 3.2: Comparison of created land cover map with RGB imagery.



**Figure 3.3:** Probability of chosen land cover class being present on the ground. This can be treated as confidence of model on its results.



# Chapter 4

## Assessing model quality

Table with quality indices:

- overall accuracy (OA) / classification error (CE)
- producer's and user's accuracy (PA, UA) / precision and recall
- F1-score
- Kappa coefficient

**Table 4.1:** Measures of overall model accuracy calculated during cross-validation/resampling process.

| Measure           | Avg. value |
|-------------------|------------|
| overall accuracy  | 0.75       |
| Kappa coefficient | 0.70       |
| precision         | 0.80       |
| recall            | 0.78       |
| F1-score          | 0.79       |

**Table 4.2:** Accuracy measures by land cover class.

| Land cover class | Precision (producer's accuracy) | Recall (user's accuracy) | F1-score |
|------------------|---------------------------------|--------------------------|----------|
| arable land      | 0.8                             | 0.75                     | 0.8      |
| grasslands       | 0.8                             | 0.70                     | 0.8      |
| forests          | 0.8                             | 0.80                     | 0.8      |
| bare land        | 0.8                             | 0.78                     | 0.8      |
| artificial land  | 0.8                             | 0.79                     | 0.8      |
| water bodies     | 0.8                             | 0.80                     | 0.8      |
| wetlands         | 0.8                             | 0.80                     | 0.8      |

# Chapter 5

## Evaluation of thermal band's impact on prediction results

### 5.1 Overall importance of thermal band

- mean temperature for every predicted land cover class
- mean importance of thermal band on each land cover class
- variable importance plots, variable profiles

**Table 5.1:** Mean value and importance of thermal band, by land cover class.

| Land cover class | Avg. value | Avg. importance |
|------------------|------------|-----------------|
| arable land      | 0.8        | 0.75            |
| grasslands       | 0.8        | 0.70            |
| forests          | 0.8        | 0.80            |
| bare land        | 0.8        | 0.78            |
| artificial land  | 0.8        | 0.79            |
| water bodies     | 0.8        | 0.80            |
| wetlands         | 0.8        | 0.80            |

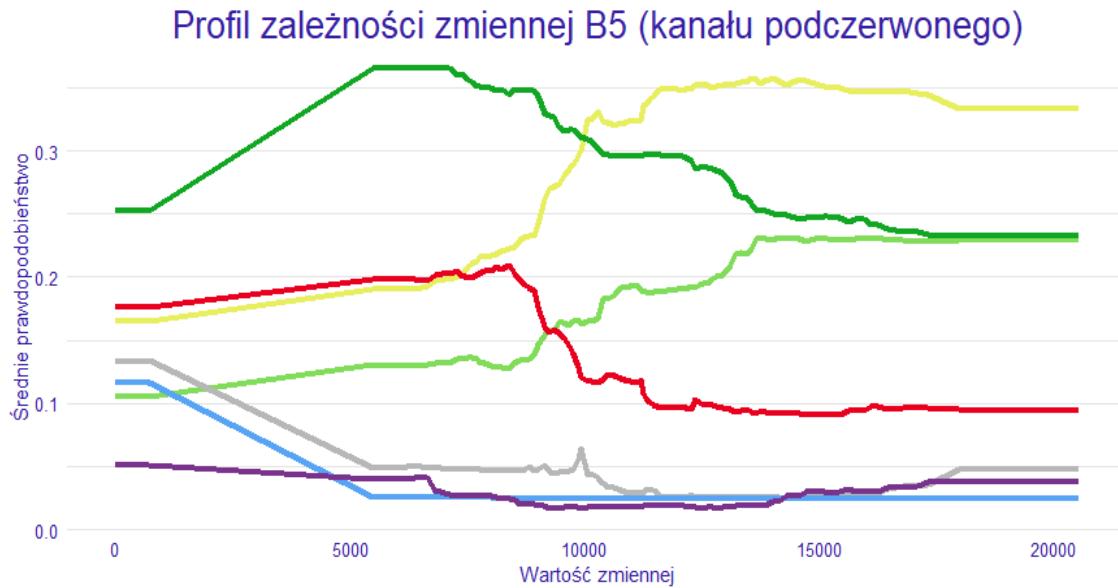


**Figure 5.1:** Variable profile for near-infrared band (B5).

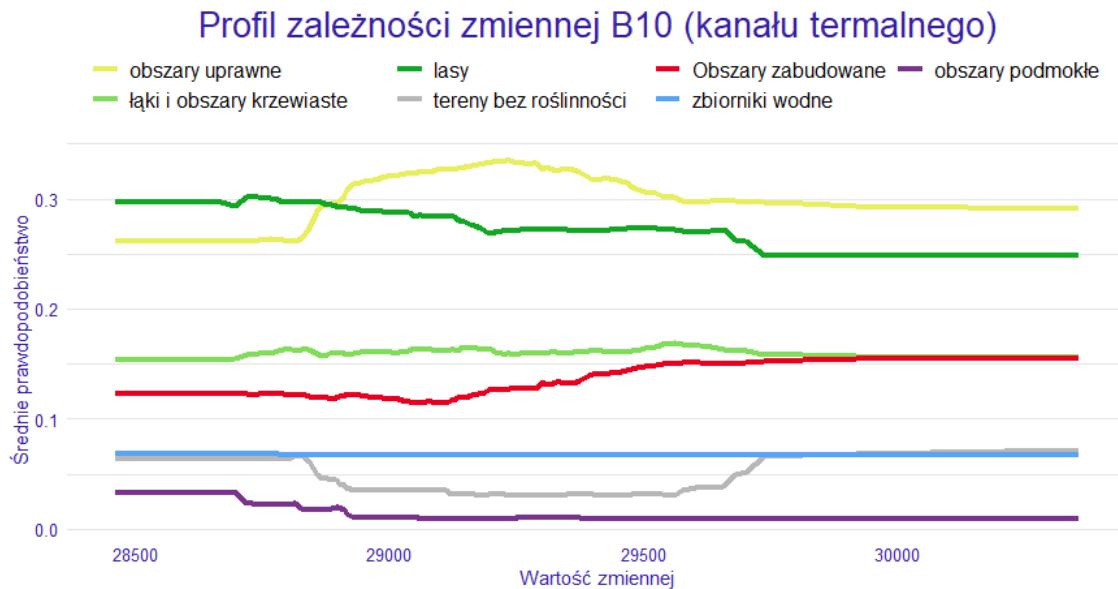


**Figure 5.2:** Variable profile for thermal band (B10)

## 5.2 Spatial distribution of thermal band's importance

- thermal band importance map (two methods: raster aggregation and interpolation of importance in LUCAS points)
- difference raster map between prediction with and without thermal band included, transition matrix (?)

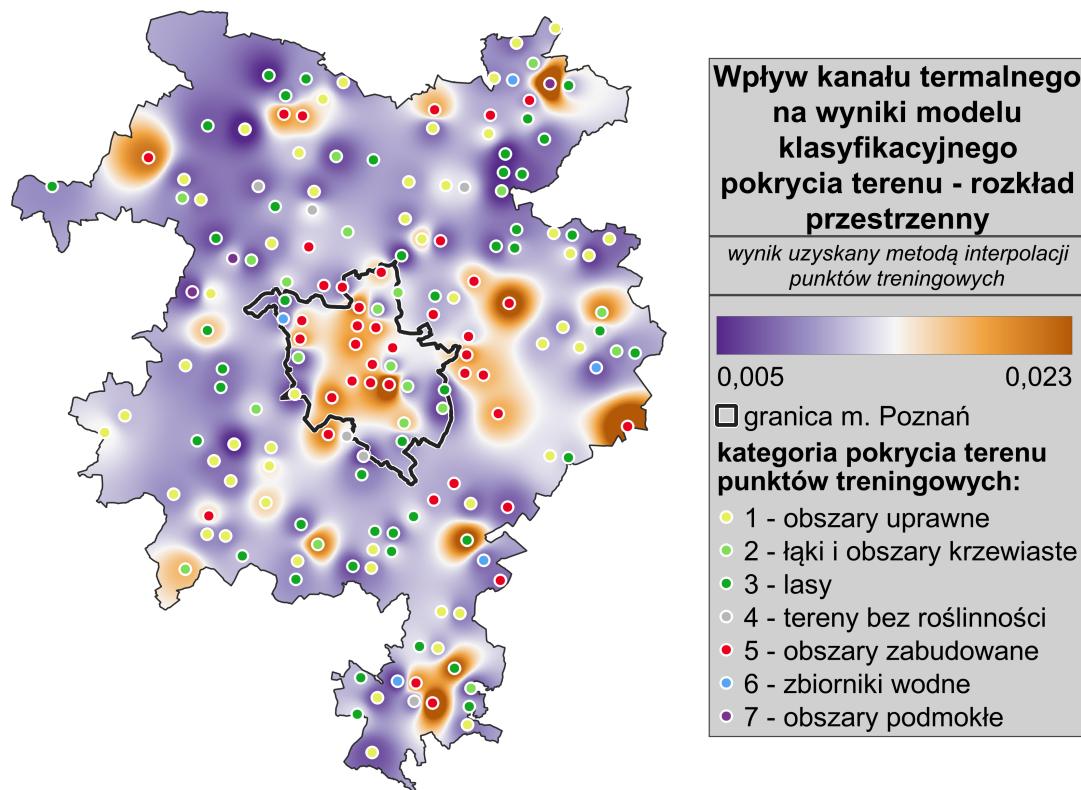


**Figure 5.3:** Thermal band importance calculated for raster cells aggregated to 1,5 km resolution.

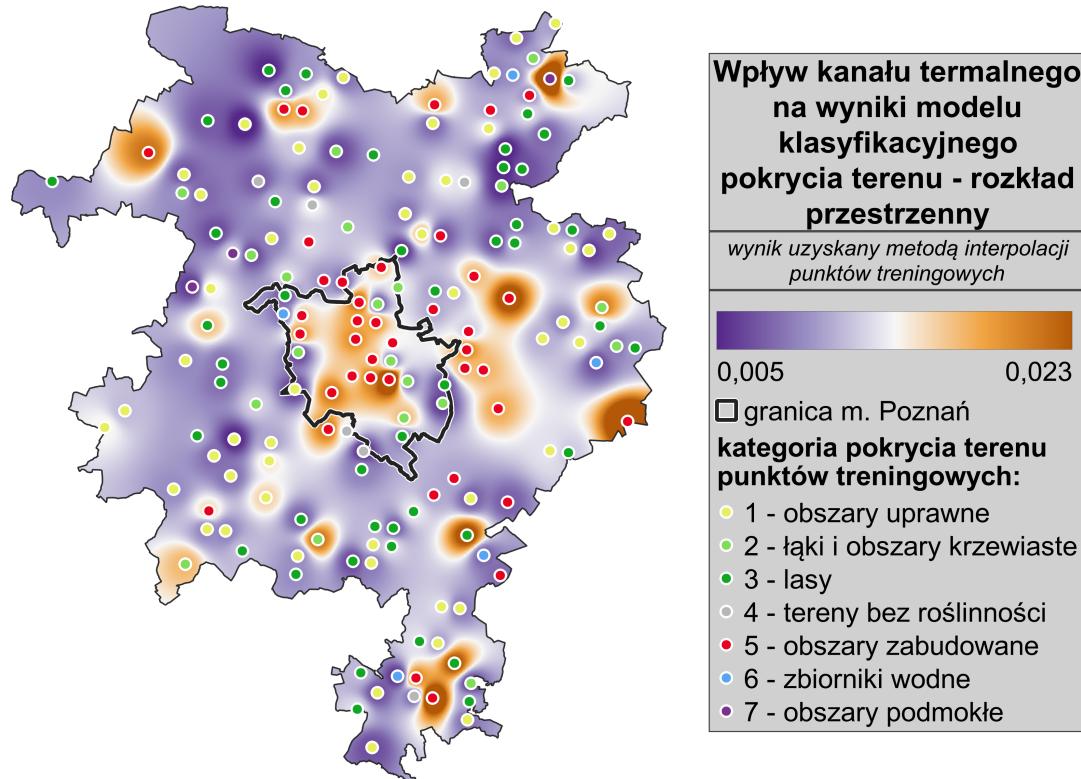


**Figure 5.4:** Thermal band importance interpolated from values on LUCAS points locations.



# Chapter 6

## Conclusion

- land cover map of Poznań metropolitan area was created, impact of thermal band on classification results was measured
- despite thermal band having low overall impact on model results, there is a strong spatial auto-correlation for its importance
- land surface temperature was especially significant for land cover classification of urban areas, it helped in identify built-up areas
- it may mean that thermal band will become increasingly important in studies on urban sprawl and suburbanisation
- better land cover maps will help in better management of metropolitan areas growth and quantifying impact of urbanisation on natural environment more precisely

---

Podsumowanie pracy jest w pewnym sensie znacznie rozbudowanym abstraktem. Należy wyliczyć i opisać osiągnięcia uzyskane w pracy dyplomowej. Tutaj jednak (w przeciwieństwie do np. rozdziału **?@sec-wprowadzenie**) należy przeходить od szczegółu do ogólnego - co zostało stworzone/określone, jak zostało to zrobione, jakie ma to konsekwencje, itd.

Ten rozdział powinien też zawierać opis kwestii, których nie udało się rozwiązać w pracy dyplomowej (i dlaczego się nie udało) oraz pomysły na przyszłe ulepszenie uzyskanych wyników lub dalsze badania.

# Bibliography

- Bengtsson, H (2021). *future: Unified Parallel and Distributed Processing in R for Everyone*. R package version 1.23.0. <https://CRAN.R-project.org/package=future>.
- Biecek, P and T Burzykowski (2021). *Explanatory Model Analysis*. Chapman and Hall/CRC, New York. <https://pbiecek.github.io/ema/>.
- Biecek, P, S Maksymiuk, and H Baniecki (2022). *DALEX: moDel Agnostic Language for Exploration and eXplanation*. R package version 2.4.0. <https://CRAN.R-project.org/package=DALEX>.
- Breiman, L (2001). Random Forests. *Machine Learning* **45**(1), 5–32.
- Brenning, A (2012). Spatial cross-validation and bootstrap for the assessment of prediction rules in remote sensing: The R package sperrorest. en. In: *2012 IEEE International Geoscience and Remote Sensing Symposium*. Munich, Germany: IEEE, pp.5372–5375. <http://ieeexplore.ieee.org/document/6352393/> (visited on 01/03/2023).
- Buck, O, C Haub, S Woditsch, D Lindemann, L Kleinewillingshöfer, G Hazeu, B Kosztra, S Kleeschulte, S Arnold, and M Hödl (2015). *Analysis of the LUCAS nomenclature and proposal for adaptation of the nomenclature in view of its use by the Copernicus land monitoring services*. [https://land.copernicus.eu/user-corner/technical-library/LUCAS\\_Copernicus\\_Report\\_v22.pdf](https://land.copernicus.eu/user-corner/technical-library/LUCAS_Copernicus_Report_v22.pdf).
- d'Andrimont, R, M Yordanov, L Martinez-Sánchez, B Eiselt, A Palmieri, P Dominici, J Gallego, HI Reuter, C Joebges, G Lemoine, and M van der Velde (2020). Harmonised LUCAS in-situ land cover and use database for field surveys from 2006 to 2018 in the European Union. en. *Scientific Data* **7**(1), 352. (Visited on 11/13/2022).
- Hijmans, RJ (2022). *terra: Spatial Data Analysis*. R package version 1.5-21. <https://rspatial.org/terra/>.

## BIBLIOGRAPHY

---

- Jiao, Y and P Du (2016). Performance measures in evaluating machine learning based bioinformatics predictors for classifications. en. *Quantitative Biology* 4(4), 320–330. (Visited on 01/03/2023).
- Kuhn, M and K Johnson (2013). *Applied Predictive Modeling*. en. New York, NY: Springer New York. <http://link.springer.com/10.1007/978-1-4614-6849-3> (visited on 12/20/2022).
- Lang, M, B Bischl, J Richter, P Schratz, and M Binder (2022). *mlr3: Machine Learning in R - Next Generation*. R package version 0.13.3. <https://CRAN.R-project.org/package=mlr3>.
- Lovelace, R, J Nowosad, and J Muenchow (2019). *Geocomputation with R*. CRC Press.
- Mahesh, B (2018). Machine Learning Algorithms - A Review. en. 9(1).
- Maksymiuk, S, P Biecek, and H Baniecki (2022). *DALEXtra: Extension for DALEX Package*. R package version 2.2.0. <https://CRAN.R-project.org/package=DALEXtra>.
- Pebesma, E (2022). *sf: Simple Features for R*. R package version 1.0-7. <https://CRAN.R-project.org/package=sf>.
- Pebesma, E and B Graeler (2021). *gstat: Spatial and Spatio-Temporal Geostatistical Modelling, Prediction and Simulation*. R package version 2.0-8. <https://github.com/r-spatial/gstat/>.
- Pflugmacher, D, A Rabe, M Peters, and P Hostert (2019). Mapping pan-European land cover using Landsat spectral-temporal metrics and the European LUCAS survey. en. *Remote Sensing of Environment* 221, 583–595. (Visited on 04/14/2022).
- Potapov, P, MC Hansen, I Kommareddy, A Kommareddy, S Turubanova, A Pickens, B Adusei, A Tyukavina, and Q Ying (2020). Landsat Analysis Ready Data for Global Land Cover and Land Cover Change Mapping. en. *Remote Sensing* 12(3), 426. (Visited on 04/07/2022).
- QGIS Development Team (2009). *QGIS Geographic Information System*. <https://www.qgis.org>.
- Qi, Y (2012). Random Forest for Bioinformatics. en.
- R Core Team (2021). *R: A Language and Environment for Statistical Computing*. R Foundation for Statistical Computing. Vienna, Austria. <https://www.R-project.org/>.

## BIBLIOGRAPHY

---

- RStudio Team (2020). *RStudio: Integrated Development Environment for R*. Boston, MA.  
<http://www.rstudio.com/>.
- Sarker, IH (2021). Machine Learning: Algorithms, Real-World Applications and Research Directions. en. *SN Computer Science* **2**(3), 160. (Visited on 12/15/2022).
- Schonlau, M and RY Zou (2020). The random forest algorithm for statistical learning. en. *The Stata Journal: Promoting communications on statistics and Stata* **20**(1), 3–29. (Visited on 12/20/2022).
- Schratz, P, J Muenchow, E Iturritxa, J Richter, and A Brenning (2019). Hyperparameter tuning and performance assessment of statistical and machine-learning algorithms using spatial data. en. *Ecological Modelling* **406**, 109–120. (Visited on 01/03/2023).
- Sekulić, A, M Kilibarda, GB Heuvelink, M Nikolić, and B Bajat (2020). Random Forest Spatial Interpolation. en. *Remote Sensing* **12**(10), 1687. (Visited on 12/20/2022).
- Shapley, LS, KJ ARROW, EW BARANKIN, D BLACKWELL, R BOTT, N DALKEY, M DRESHER, D GALE, DB GILLIES, I GLICKSBERG, O GROSS, S KARLIN, HW KUHN, JP MAYBERRY, JW MILNOR, TS MOTZKIN, J VON NEUMANN, H RAIFFA, LS SHAPLEY, M SHIFFMAN, FM STEWART, GL THOMPSON, and RM THRALL (1953). “A VALUE FOR n-PERSON GAMES”. In: *Contributions to the Theory of Games (AM-28), Volume II*. Ed. by HW Kuhn and AW Tucker. Princeton University Press, pp.307–318.  
<http://www.jstor.org/stable/j.ctt1b9x1zv.24> (visited on 01/09/2023).
- Sohil, F, MU Sohali, and J Shabbir (2022). An introduction to statistical learning with applications in R: by Gareth James, Daniela Witten, Trevor Hastie, and Robert Tibshirani, New York, Springer Science and Business Media, 2013, \$41.98, eISBN: 978-1-4614-7137-7. en. *Statistical Theory and Related Fields* **6**(1), 87–87. (Visited on 01/03/2023).
- Strumbelj, E and I Kononenko (2010). An Efficient Explanation of Individual Classifications using Game Theory. en.
- Tobler, WR (1970). A Computer Movie Simulating Urban Growth in the Detroit Region. en. *Economic Geography* **46**, 234. (Visited on 01/04/2023).
- Varga, OG, Z Kovács, L Bekő, P Burai, Z Csatárинé Szabó, I Holb, S Ninsawat, and S Szabó (2021). Validation of Visually Interpreted Corine Land Cover Classes with Spectral Values of Satellite Images and Machine Learning. en. *Remote Sensing* **13**(5), 857. (Visited on 04/07/2022).

## BIBLIOGRAPHY

---

- Wickham, H (2021). *tidyverse: Tidy Messy Data*. R package version 1.1.4. <https://CRAN.R-project.org/package=tidyr>.
- Wickham, H, W Chang, L Henry, TL Pedersen, K Takahashi, C Wilke, K Woo, H Yutani, and D Dunnington (2021). *ggplot2: Create Elegant Data Visualisations Using the Grammar of Graphics*. R package version 3.3.5. <https://CRAN.R-project.org/package=ggplot2>.
- Wickham, H, R François, L Henry, and K Müller (2022). *dplyr: A Grammar of Data Manipulation*. R package version 1.0.10. <https://CRAN.R-project.org/package=dplyr>.
- Wright, MN, S Wager, and P Probst (2021). *ranger: A Fast Implementation of Random Forests*. R package version 0.13.1. <https://github.com/imbs-hl/ranger>.
- Yang, L and A Shami (2020). On Hyperparameter Optimization of Machine Learning Algorithms: Theory and Practice. en. *Neurocomputing* **415**. arXiv:2007.15745 [cs, stat], 295–316. (Visited on 01/02/2023).